J Math Chem (2010) 47:1248–1262
DOI 10.1007/s10910-009-9649-7

ORIGINAL PAPER

# An analysis of nonlinear ion transport problem including arbitrary valences of oxidized and reduced species

**Alemdar Hasanov · Burhan Pektaş · Umit Kadiroglu**

Received: 30 January 2009 / Accepted: 25 November 2009 / Published online: 5 December 2009
© Springer Science+Business Media, LLC 2009

**Abstract** The nonlocal identification problem related to nonlinear ion transport model including diffusion and migration is studied. Ion transport is assumed to be superposition of diffusion and migration under the influence of an electric field. Mathematical modeling of the experiment leads to an identification problem for a strongly nonlinear parabolic equation with nonlocal additional condition. It is shown that the nonlocal identification problem can be reduced to the initial-boundary value problem for nonlinear parabolic equation. Iteration method for numerical solution of this problem is proposed. Numerical results and their interpretation are presented for wide class of materials, including various values of valences and diffusivities of oxidized and reduced species.

**Keywords** Nonlinear ion transport · Diffusion and migration · Reduced parabolic problem · Total charge · Current response · Iteration scheme

## 1 Introduction

Transport mechanisms in electrochemical systems are frequently studied by electrochemical transient techniques, using various linear parabolic equations, including diffusion or diffusion-migration, or diffusion-convection processes. The most used equation is the Cottrell equation, which was derived for linear initial-boundary value problems (IBVP) based on Nernst–Planck equation. These problems were examined

A. Hasanov · B. Pektaş (✉)
Department of Mathematics and Computer Sciences, Izmir University, 35340 Uckuyular, Izmir, Turkey
e-mail: burhanps@gmail.com

U. Kadiroglu
Department of Chemistry, Kocaeli University, Umuttepe Campus, 41380 Izmit-Kocaeli, Turkey

with an open circuited planar electrode, large enough not to be affected by the edge effects in contact with a semi-infinite layer of electrolyte solution containing uniformly distributed electroactive species, one-dimensional geometry and purely diffusional transport [1,2]. Cottrell showed that is the case when a potential applied to the cell the resulting current response, known as Cottrellian is proportional to $1/\sqrt{t}$. This result has been confirmed both theoretically and experimentally under steady-state conditions. However, there are some essential deviations from the Cottrellian behavior due to the complex electrochemical kinetics as shown in many experimental works [3,4]. In order to overcome such a problem, in recent years many mathematical and computational models related to the electrochemical transport problem have been studied [5–12]. Mostly using the digital simulation techniques, these studies are based on linear models for the transport of the electroactive species. Lantelme et al. [5] studied mathematical analysis of the diffusion process to examine the validity of the classical treatment when the diffusion coefficient depends on the concentration. Bieniasz [6] studied the chronoamperometry of a charge neutralization process under conditions of linear migration and diffusion. Churikov et al. [7] studied both theoretically and experimentally transfer process of lithium intercalation, using pulse methods. Vorotyntsev et al. [8] analyzed chronoamperometric curves after small amplitude potential steps for the model linear diffusion of the electroactive species.

On the other hand, Cohn et al. [9] derived a nonlinear initial boundary value problem with a nonlocal condition to model mass and charge transport in a chronoamperometric experiment. They considered both diffusion and migration. The latter component of the total flux leads to an additional nonlinearity in the transport equations. They proved that the initial boundary value problem has a unique similarity solution. Hasanov [10] and Hasanov et al. [11] studied some numerical methods for the similarity solution of nonlocal identification problem. Some special cases of the nonlinear initial boundary value problem with a nonlocal condition have been studied by Hasanov et al. [13,14].

In this paper, we extend the mathematical method, proposed in [14] to obtain the numerical solution of the nonlinear ion transport problem, including both diffusion and migration, without the restrictions, imposed in [14]. In the next section, the mathematical model of the nonlinear nonlocal identification problem related to ion transport is derived. Reduction method for the identification problem in the case of arbitrary values of valences and diffusivities of oxidized and reduced species, is proposed in Sect. 3. The nonlinear finite-difference scheme for the reduced problem, and iteration algorithm are given in Sect. 4. Computational results and comparative analysis with the previous model are given in Sect. 5. The final Sect. 6 contains some conclusions.

## 2 The mathematical model including arbitrary valences of oxidized and reduced species

The nonlinear mathematical model of mass and charge transport in a controlled potential experiment, for the case of two-species migrating under the influence of the electric field, have first been derived by Cohn et al. [9]. In this model, ion transport is

assumed to be superposition of diffusion and migration, and there is only oxidized species before the potential applied. In perspective of this scaled model, the following identification problem for the nonlinear parabolic, with the additional nonlocal condition is obtained:

$$\begin{cases} u_t = (g(u)u_x)_x + q'(t)h(u)_x, & (x,t) \in \Omega_\infty := (0,\infty)\times(0,\infty), \\ u(x,0) = 0, & x > 0, \\ u(0,t) = 1, & t > 0; \end{cases} \tag{1}$$

$$q(t) = \int_0^\infty u(x,t)dx, \quad t \geq 0. \tag{2}$$

Here the functions $u(x,t)$ and the coefficient $q(t)$ are defined to be the concentration of reduced species and the scaled total charge. According to this scaled model, the concentration functions $u(x,t)$ satisfies the following condition: $0 \leq u(x,t) \leq 1$.

The pair of functions $\langle u(x,t), q(t)\rangle$ will be defined as a solution of the nonlocal identification problem (1)–(2).

The coefficients $g(u) > 0$ and $h(u)$ are related to diffusion and migration in the ion transport, and have the forms [9]:

$$g(u) := \frac{z_0 + (z_r - z_0)u}{z_0 + (z_r\kappa - z_0)u}, \quad h(u) := \frac{\kappa u}{z_0 + (z_r\kappa - z_0)u}. \tag{3}$$

Here and below the dimensionless parameters $\kappa := D_r/z_o$ and $z_r, z_0$ denote the diffusivity ratio, and valences of the reduced and oxidized species, respectively.

Due to mathematical as well as computational difficulties related to solving the nonlinear and nonlocal identification problem (1)–(2), as a first attempt, Hasanov et al. [14] studied this mathematical model under the following assumptions:

(A1) $u(\infty,t) = u_x(\infty,t) = 0, \quad \forall t > 0;$
(A2) $z_r D_r = z_o D_o$

Assumption (A1) is based on experimental and theoretical results of various authors (see, [9] and references therein), obtained for the nonlinear model (1)–(2). Specifically, these results show that for a fixed time $t \in (0,\infty)$, the concentration function $u(x,t)$ and its partial derivative $u_x(x,t)$ decreases rapidly to zero, as $x \to \infty$, for all $t > 0$. Although the assumption (A2) makes some restriction for values of diffusivities $D_r$ and $D_o$, it permits one to simplify the nonlinearity of the parabolic equation (1). Under the assumption (A2) the functions $g(u)$ and $h(u)$, defined by (3), have the following forms:

$$g(u) := 1 + \left(\frac{z_r}{z_o} - 1\right)u, \quad h(u) := \frac{1}{z_r}u.$$

As a result, the second nonlinear term $h(u)_x$ in the parabolic equation (1) becomes linear, $h(u)_x := u_x/z_r$, and the equation has the form:

$$u_t = ([1 + (z_r/z_o - 1)u]u_x)_x + q'(t)u_x/z_r, \quad (x,t) \in \Omega_\infty,$$

We will refer to here this nonlinear model as *Model (N0)*.

In this study we consider the general case, assuming only that $u(x,t) \to 0$, as $x \to \infty$, which is a quite real assumption from the point of view an experiment. This model will be defined here as the *Model (N1)*.

To analyze the Model (N1), as well as the differences of these nonlinear models, we will derive energy identity, corresponding to both models. For this aim, let us multiply the both sides of the nonlinear parabolic equation (1) by the function $u(x,t)$, and then integrate on $\Omega_t := (0,\infty) \times (0,t)$. Applying integration by parts, using elementary transformations and taking into account $h(u)_x = h'(u)u_x$, we obtain:

$$\frac{1}{2}\int_0^\infty u^2(x,t)dx + \int_0^t\int_0^\infty g(u)u_x^2(x,\tau)dxd\tau =$$
$$\int_0^t [g(u(\infty,\tau))u_x(\infty,\tau)u(\infty,\tau) - g(u(0,\tau))u_x(0,\tau)u(0,\tau)]d\tau$$
$$+\frac{1}{2}\int_0^t q'(\tau)\int_0^\infty h'(u)(u^2(x,\tau))_x dxd\tau, \quad t > 0.$$

We use here the initial and boundary conditions $u(x,0) = 0, u(0,t) = 1$, the boundedness condition at infinity $u(\infty,t) = 0, t > 0$ and the condition $g(u(0,t)) = g(1) = 1/\kappa$. Then we get:

$$\frac{1}{2}\int_0^\infty u^2(x,t)dx + \int_0^t\int_0^\infty g(u)u_x^2(x,\tau)dxd\tau =$$
$$-\frac{1}{\kappa}\int_0^t u_x(0,\tau)d\tau + \frac{1}{2}\int_0^t q'(\tau)\int_0^\infty h'(u)(u^2(x,\tau))_x dxd\tau, \quad t > 0, \tag{4}$$

where

$$h'(u) := \frac{\kappa z_o}{[z_o + (z_r\kappa - z_o)u]^2}. \tag{5}$$

The left hand side of (4), which expresses the energy of the system, is defined to be the energy integral. The energy identity (4) provides further insight into the solution the nonlinear problem (1)–(2). Moreover, this identity permits one to predict some distinguished features of the energy integral, corresponding to models (N0) and (N1).

The first result follows from the positivity of the energy integral. According to the definition, the flux at $x = 0$ is defined to be $\varphi_L(0,t) := -(g(u)u_x)_{x=0}$. With the definition (3) of the function $g(u)$, we have $g(u(0,t)) = g(1) = 1/\kappa$, and hence

$$\varphi_L(0,t) := -(g(u)u_x)_{x=0} = -u_x(0,t)/\kappa.$$

This means that the first integral on the right hand side of the energy identity (4) is the total flux

$$\Phi_L(0,t) := -\int_0^t (g(u)u_x(x,\tau))_{x=0} d\tau, \tag{6}$$

at the electrode surface $x = 0$ during the time $t > 0$. From the positivity of the energy integral (4) we get the following

**Proposition 2.1** *The lower bound of total flux at the electrode surface $x = 0$ during the time $t > 0$ is estimated via the integral, generated by the migration term $h(u)_x$, as follows:*

$$\Phi_L(0,t) > -\frac{1}{2}\int_0^t q'(\tau)\int_0^\infty h'(u)(u^2(x,\tau))_x dx d\tau, \quad t > 0. \tag{7}$$

In the case of the Model (N0), the above integral, generated by the migration term $h(u)_x$, can be simplified due to the condition $z_r D_r = z_o D_o$ (assumption (A2)), which imply $z_o = \kappa z_r$. Substituting this in (5) we get $h'(u) = 1/z_r$. Using this in the energy identity (4) we get:

$$\frac{1}{2}\int_0^\infty u^2(x,t)dx + \int_0^t\int_0^\infty g(u)u_x^2(x,\tau)dxd\tau =$$
$$-\frac{1}{\kappa}\int_0^t u_x(0,\tau)d\tau + \frac{1}{2z_r}\int_0^t q'(\tau)\int_0^\infty (u^2(x,\tau))_x dxd\tau, \quad t > 0.$$

Calculating the last right hand side integral, we finally obtain that the energy identity, corresponding to the Model (N0), is as follows:

$$\frac{1}{2}\int_0^\infty u^2(x,t)dx + \int_0^t\int_0^\infty g(u)u_x^2(x,\tau)dxd\tau = -\frac{1}{\kappa}\int_0^t u_x(0,\tau)d\tau - \frac{1}{2z_r}q(t), \ t > 0. \tag{8}$$

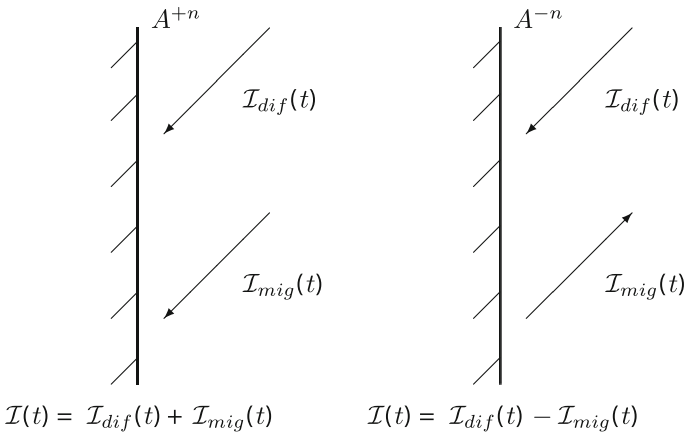


**Fig. 1** Signs of valences and corresponding current responses

**Proposition 2.2** *Let condition $z_r D_r = z_o D_o$ hold. Then lower bound of total flux at the electrode surface $x = 0$ during the time $t > 0$ is estimated via the scaled total charge $q(t)$, as follows:*

$$\Phi_L(0,t) > \frac{1}{2z_r} q(t), \quad t > 0. \tag{9}$$

Let us explain interpretation of the above results. By definition (see, [1,9]) the time-dependent current response $\mathcal{I}(t)$ is defined via the ion fluxes $J_o$, $J_r$ and the valences $z_o, z_r$ as follows: $\mathcal{I}(t) = -n\mathcal{F}A(z_o J_o + z_r J_r)$, where $n$ is the number of electrons gained by an ion reduction, $\mathcal{F}$ is Faraday's constant, and $A$ is the surface area of the electrode. For the negative values ($z_r < 0$) of the valences of the reduced species, currents corresponding to diffusion ($\mathcal{I}_{\text{diff}}(t)$) and migration ($\mathcal{I}_{\text{migr}}(t)$), are in the same direction (Fig. 1). This means that cationic species react at cathode and anionic species react at anode. For positive values ($z_r > 0$) currents of diffusion and migration are in opposite signs, which means that anions are reduced at cathode. In the first case, the total current response $\mathcal{I}(t)$ at the electrode surface will be sum of the diffusion and migration components: $\mathcal{I}(t) = \mathcal{I}_{\text{diff}}(t) + \mathcal{I}_{\text{migr}}(t)$. Thus at the electrode surface both diffusional and migrational fluxes contribute to the total flux. For the other case ($z_r, z_0 < 0$) the total current response at the electrode surface will be difference between diffusional and migrational components. Thus, at the electrode surface diffusional flux contributes to the total flux. In addition the migrational flux contributes to the total flux in the bulk solution (far away from the electrode).

## 3 Reducing the nonlinear identification problem (1)–(2)

We are going to reduce the identification problem (1)–(2), applying the approach proposed in [14]. For this aim, we need to eliminate the additional condition (2), and reduce the identification problem (1)–(2) to the initial-boundary value problem for

a strongly nonlinear parabolic equation. Integrating the both sides of the parabolic equation (1) on $\Omega_t$ we obtain:

$$\int_0^\infty u(x,t)dx = \int_0^t [g(u(\infty,\tau))u_x(\infty,\tau) - g(u(0,\tau))u_x(0,\tau)]d\tau + \int_0^t q'(\tau)[h(u(\infty,\tau)) - h(u(0,\tau))]d\tau.$$

On the left hand side we use Eq. (2). To calculate the terms under the right hand side integrals we use the conditions:

$$g(u(\infty,t)) = g(0) = 1, \quad g(u(0,t)) = g(1) = 1/\kappa;$$
$$h(u(\infty,t)) = h(0) = 0, \quad h(u(0,t)) = h(1) = 1/z_r,$$

taking into account formulas (3) for the coefficients $g(u)$ and $h(u)$. Then we have:

$$\int_0^\infty u(x,t)dx = \int_0^t [u_x(\infty,\tau) - \frac{1}{\kappa}u_x(0,\tau)]d\tau - \frac{1}{z_r}\int_0^t q'(\tau)d\tau.$$

Since $q(0) = 0$, due to the initial condition $u(x,0) = 0$ the above equation yields:

$$q(t) = \int_0^t [u_x(\infty,\tau) - \frac{1}{\kappa}u_x(0,\tau)]d\tau - \frac{1}{z_r}q(t).$$

Solving this equation with respect to $q(t)$ we obtain:

$$q(t) = \frac{z_r}{1+z_r}\left[\int_0^t g(u(\infty,\tau))u_x(\infty,t)d\tau - \int_0^t g(u(0,\tau))u_x(0,t)d\tau\right]. \quad (10)$$

The term under the first right hand side integral is equal to $-\varphi_R(\infty,t)$, where $\varphi_R(\infty,t) := -(g(u)u_x(x,\tau))_{x=\infty}$ is the flux at $x = \infty$, according to the definition. Then the total flux at $x = \infty$ during the time $t > 0$ will be defined as follows:

$$\Phi_R(\infty,t) := -\int_0^t (g(u)u_x(x,\tau))_{x=\infty}d\tau = -\int_0^t u_x(\infty,\tau))d\tau. \quad (11)$$

Therefore taking into account also (6) we may rewrite relationship (10) in the following form:

$$q(t) = \frac{z_r}{1+z_r}[\Phi_L(0,t) - \Phi_R(\infty,t)]. \tag{12}$$

**Proposition 3.1** *The scaled total charge $q(t)$ is proportional to the difference of the left ($\Phi_L(0,t)$) and right ($\Phi_R(0,t)$) total fluxes during the time $t > 0$.*

Comparing this result with [14], we conclude that not only the left flux has an influence to the value of the scaled total charge $q(t)$, but also the right flux needs to be taken into account.

Differentiating the both sides of (10) yields

$$q'(t) = \frac{z_r}{1+z_r}\left[u_x(\infty,t) - \frac{1}{\kappa}u_x(0,t)\right]. \tag{13}$$

Using here the above definitions of the fluxes $\varphi_L(0,t)$ and $\varphi_R(\infty,t)$, at $x = 0$ and $x = \infty$, respectively, and the relationship

$$q'(t) = \frac{z_r}{n\mathcal{F}S_e u_0}\mathcal{I}(t)$$

between the scaled total charge and current response $\mathcal{I}$ we obtain the following result.

**Proposition 3.2** *The current response $\mathcal{I}(t)$ is proportional to the difference of the left $\varphi_L(0,t)$ and right $\varphi_R(\infty,t)$ fluxes at $x = 0$ and $x = \varphi$, respectively:*

$$\mathcal{I}(t) = \frac{n\mathcal{F}S_e u_0}{1+z_r}[\varphi_L(0,t) - \varphi_R(\infty,t)]. \tag{14}$$

Finally substituting in the parabolic equation (1) formula (13) for $q'(t)$, we obtain the following:

**Proposition 3.3** *The nonlocal identification problem (1)–(2) is equivalent to the following initial-boundary value problem:*

$$\begin{cases} u_t = (g(u)u_x)_x + \frac{z_r}{1+z_r}\left[u_x(\infty,t) - \frac{1}{\kappa}u_x(0,t)\right]h(u)_x, & (x,t) \in \Omega_\infty, \\ u(x,0) = 0, & x > 0, \\ u(0,t) = 1, & t > 0. \end{cases} \tag{15}$$

Since $h(u)_x = h'(u)u_x$ we may introduce for subsequent convenience the functions

$$Q(t;u) = \frac{z_r}{1+z_r}\left[u_x(\infty,t) - \frac{1}{\kappa}u_x(0,t)\right], \quad H(u) = h'(u), \tag{16}$$

and rewrite the transformed problem (15) in the following form

$$\begin{cases} u_t = (g(u)u_x)_x + Q(t;u)H(u)u_x, & (x,t) \in \Omega_\infty, \\ u(x,0) = 0, & x > 0, \\ u(0,t) = 1, & t > 0, \end{cases} \tag{17}$$

for subsequent convenience of iteration process for the nonlinear parabolic equation.

## 4 Numerical algorithm and test examples

For linearization of the reduced problem (17) we propose the following iteration algorithm:

$$\begin{cases} u_t^{(n+1)} = \left(g(u^{(n)})u_x^{(n+1)}\right)_x \\ \quad +Q(t,u^{(n)})H(u^{(n)})u_x^{(n+1)}, & (x,t) \in \Omega_\infty, \\ u^{(n+1)}(x,0) = 0, & x > 0, \\ u^{(n+1)}(0,t) = 1, & u^{(n+1)}(\infty,t) = 0, \ t > 0. \end{cases} \tag{18}$$

Here $u^{(n)} = u^{(n)}(x,t)$ represents the $n$th iteration for the approximate solution. In the presented iteration algorithm, the values of the diffusion and migration coefficients are taken from the previous iteration. The condition

$$\|u^{(n+1)} - u^{(n)}\|_\infty < \epsilon_{stop} \tag{19}$$

is defined to be the stopping criteria for the iteration process (18), where the parameter $\epsilon_{stop} > 0$ is defined to be the stopping parameter.

For the numerical solution of the linearized (reduced) problem (18), the following uniform space and time grids are defined:

$$\begin{aligned} \overline{w}_h &= \{x_i \in [0,L] : x_i = ih_x; \quad i = \overline{0,N_x}, \quad h_x = L/N_x\}, \\ \overline{w}_\tau &= \{t_j \in [0,T] : t_j = jh_t; \quad j = \overline{0,N_t}, \quad h_t = T/N_t\}, \end{aligned}$$

where the numbers $L > 0$, $T > 0$ are chosen to be large enough. We apply following implicit monotone finite difference scheme (see [15]) for the numerical solution of the linearized problem (18):

$$\begin{cases} \frac{y_i^{j+1} - y_i^j}{\tau} = \frac{1}{h}\left(g_{i+0.5}^{j+1}\frac{y_{i+1}^{j+1} - y_i^{j+1}}{h} - g_{i-0.5}^{j+1}\frac{y_i^{j+1} - y_{i-1}^{j+1}}{h}\right) \\ \quad +Q^{j+1}H_i^{j+1}\left(\frac{y_{i+1}^{j+1} - y_{i-1}^{j+1}}{2h}\right), \\ i = \overline{1,N_x - 1}, \ j = \overline{0,N_t - 1}, \\ y_0^j = 1, \ y_{N_x}^j = 0, \quad j = \overline{0,N_t}, \\ y_i^0 = 0, \quad i = \overline{0,N_x}, \end{cases} \tag{20}$$

**Table 1** Numerical results for the problem (21) on different grids and optimal values of the grid parameters $h,\ \tau$

| $h(N_x)$ | $\tau\ (N_t)$ | $R := \tau/h^2$ | Iter. number | $\varepsilon_u := \|u - y\|_\infty$ |
|---|---|---|---|---|
| 0.25 (21) | 0.25 (21) | 4 | 5 | $2.5 \times 10^{-2}$ |
| 0.125 (41) | 0.125 (41) | 8 | 5 | $1.2 \times 10^{-2}$ |
| 0.125 (41) | 0.0625 (81) | 4 | 5 | $6.9 \times 10^{-3}$ |
| **0.0625 (81)** | **0.02 (251)** | **5.12** | **6** | $\mathbf{2.2 \times 10^{-3}}$ |
| 0.1 (51) | 0.02 (251) | 2 | 5 | $2.6 \times 10^{-3}$ |
| **0.0313 (161)** | **0.02 (251)** | **20.4** | **6** | $\mathbf{2.0 \times 10^{-3}}$ |

where $y_i^j := u^{(n)}(x_i, t_j)$, $g_i^j := g(y_i^j)$, $H_i^j := H(y_i^j)$, $Q^j := Q(y^j)$. For calculating of the integral in Eq. (2) Simpson's numerical integration formula is used.

For linear problems this scheme has the accuracy $O(h^2 + \tau)$ on the uniform grid $W_{ht} = \overline{w}_h \times \overline{w}_\tau$ [15].

To verify an effectiveness of the iteration process, as well as an accuracy of the finite difference scheme, the following test example is realized. For the given coefficients $g(u) = 1 + u$, $h(u) = 1 - u$ and the function $Q(t) = 1/\sqrt{t}$, the exact solution $u(x, t) = t \exp(-x^2 - t)$ of the problem

$$\begin{cases} u_t = (g(u)u_x)_x + Q(t)h(u)_x + F(x,t), & (x,t) \in (0,L) \times (0,T), \\ u(x,0) = \phi(x), & x \in\in (0,L), \\ u(0,t) = \mu(t), & t \in (0,T), \end{cases} \tag{21}$$

is defined by appropriately choosing the right side term $F(x, t)$. Here $\phi(x) = 0, \mu(t) = t \exp(-t)$, and $L = 5, T = 5$. The scheme (20) is applied to the test problem (21), by using various values of grid parameters $h$ and $\tau$. Results are given in Table 1. For the value $\epsilon_{\text{stop}} = 10^{-4}$ of parameter defined by (19), the number of iterations is almost independent, and for all variety of grid parameters is about $5 \div 6$, as table shows. Optimal grid parameters (bold-faced characters in the table) are defined by the sup-norm error $\varepsilon_u := \|u - y\|_\infty$, between the exact and numerical solutions.

Figure 2 shows behavior of the approximate numerical solution $y$ obtained for 6 iterations, and its traces corresponding to different times $t_i > 0$. The sup-norm error here is obtained as $\varepsilon_u = 2.0 \times 10^{-3}$ for the optimal grid parameters $h = 0.0313,\ \tau = 0.02$. These results show that the accuracy of scheme (20) is high enough. The optimal grid parameters $h = 0.0313,\ \tau = 0.02$ are used in subsequent computational experiments.

Experimental and theoretical results show that [9] for a fixed $t \in (0, \infty)$ the function $u(x, t)$ and its partial derivative $u_x(x, t)$ decreases rapidly and tends to zero, as $x \to \infty$. The goal of the next computational experiment is to illustrate the behavior of the the right flux $\varphi_R(t) :\approx -(g(u(x,t))u_x(x,t))_{x=L} \equiv 1 \cdot u_x(L,t) = u_x(L,t), t > 0$, and observe the behavior of the flux in increasing values of the parameter $L > 0$.

For this aim the reduced problem (15) is solved by the iteration scheme (20), for the following values of the physical parameters: $z_r = 2$, $z_0 = 3$ and $\kappa = 5$, which means $\kappa = D_r/D_o \neq z_0/z_r$ (Model (N1)). For the value $T = 10$ of the final time parameter,

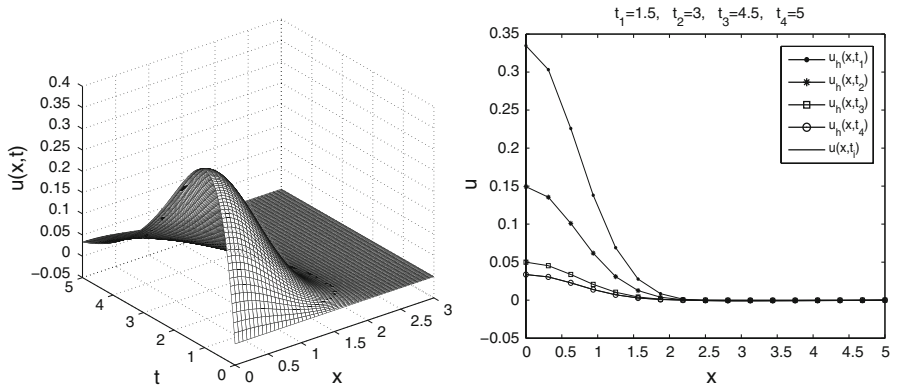


**Fig. 2** Numerical solution of the nonlinear problem (21) and its sections corresponding to different times $t_i > 0, i = 1, 2, 3, 4$

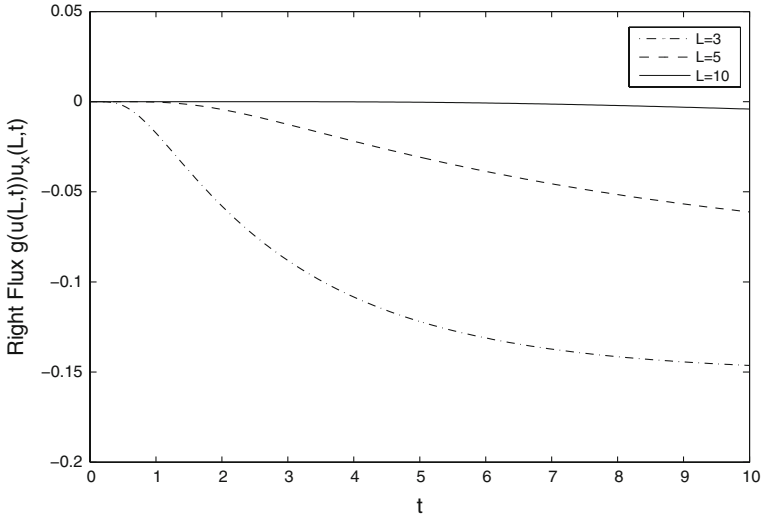


**Fig. 3** The right flux $\varphi_R(t)$ goes to zero when $L > 0$ increases

the following increasing values of the length parameter is used: $L = 3;\ 5;\ 10$. Figure 3 shows the approximate numerical results for the right flux $\varphi_R(t)$. For the values $L = 3$ and $L = 5$, the only close to the final time $T > 0$ values of the right flux $\varphi_R(t)$ are almost zero. However, for the value $L = 10$, the right flux $\varphi_R(t)$ is zero for all values of $t > 0$. Hence, errors arising due to the assumption (A1) in the Model (N0) can be neglected when $L \geq 10$. For the values $L = 1 \div 10$, an influence of the right flux $\varphi_R(t)$ needs to be taken into account. This, in particular, means that for these values the Model (N0) is not accurate.

## 5 Computational experiments based the Model (N1) and comparative analysis of the Models (N0) and (N1)

The first series of computational experiments are related to the behavior of the concentration function $u(x,t)$ with respect to the time $t \in [0,5]$ and space $x \in [0,5]$ variables, for different admissible values $z_0$ and $z_r$ of the valences of oxidized and reduced species. For this aim the nonlinear problem (15) is solved by the above iteration algorithm, with the coefficients $g(u)$ and $h(u)$, given by formulas (3), with $\kappa = 5$. For the values $(z_0, z_r) = (-2,-3); (-3,-4); (2,1); (3,2)$ of valences the numerical solutions are plotted in Fig. 4. For a fixed time $t > 0$, the numerical solution $y$ decreases rapidly and monotonically on the space interval $[0,5]$ in all cases, the figure shows. Further, in all these cases concentration function $u(x,t)$ is a smooth one. These results agree with previous theoretical and experimental results (see, [1,9,16]).

As Fig. 5 shows, when the diffusion coefficient of reduced species is smaller than the diffusion coefficient of oxidized species ($D_r < D_o$), flux increases with time. This leads to increasing of the corresponding total charge function $q(t)$ (line $\circ\ \circ\ \circ$). Moreover, in this case $q(t) > \sqrt{t}$. When $D_r = D_o$, the total charge function $q(t)$ is almost same with the function $\sqrt{t}$ (solid line). However, by increasing the values of the diffusion coefficient of reduced species, the total charge function $q(t)$ decreases. This means that at the electrode surface, charge is mainly carried out by oxidized species. In terms of the diffusivity ratio $\kappa := D_r/D_o$ these results can be formulated as follows: if $q[\kappa_n]$ and $q[\kappa_m]$ are total charge functions corresponding to the diffusivity ratios $\kappa_n$ and $\kappa$, then $\kappa_n > \kappa_m$ implies $q[\kappa_n] < q[\kappa_m]$. Therefore, the mapping $\kappa \mapsto q(t)$ is an antitone one.

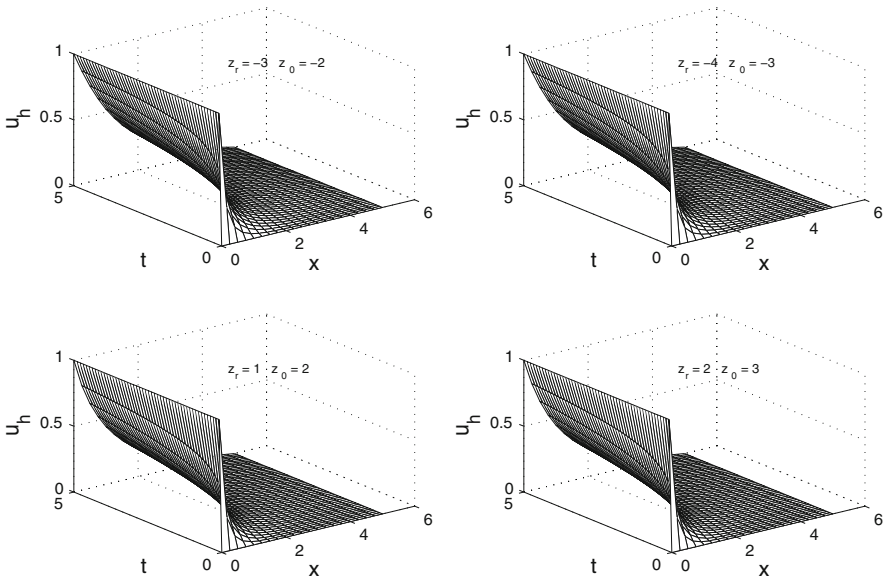


**Fig. 4** The numerical solutions of the nonlinear problem (15) for different values of valences of the oxidized and reduced species

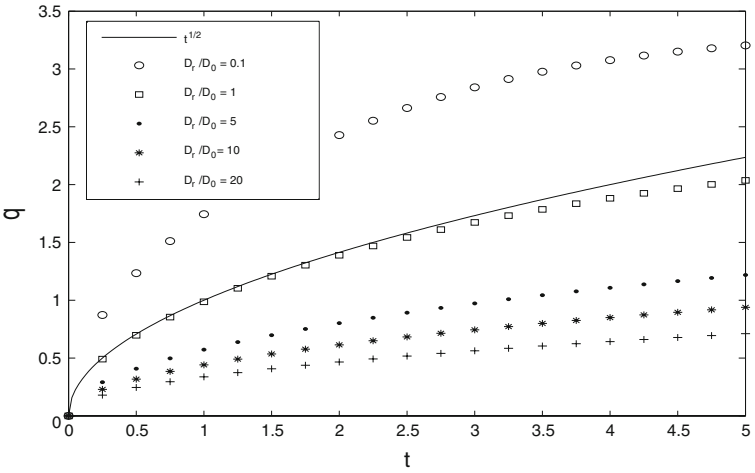


**Fig. 5** Behavior of the scaled total charge function $q(t)$ depending on diffusivity of reduced species

To compare the Models (N0) and (N1), the iteration algorithm (18) is applied to the reduced problem (15) and to the reduced problem

$$\begin{cases} u_t = (g(u)u_x)_x - \frac{1}{(1+z_r)\kappa} u_x(0,t)u_x, & (x,t) \in \Omega_T, \\ u(x,0) = 0, & x \in (0,L), \\ u(0,t) = 1, \;\; u(L,t) = 0, & t \in (0,T], \end{cases} \tag{22}$$

proposed in [14] (Model (N0)). The scaled total charge $q(t)$ is calculated only via the total flux at $x = 0$, according the Model (N0) (see, formula (16), in [14]):

$$q(t) = \frac{z_r}{1+z_r} \Phi_L(0,t). \tag{23}$$

Numerical results corresponding to different values of physical (valences and diffusivities) as well as geometric (length $L > 0$) parameters, are presented Fig. 6. In the left figure $L = 5$ and deviation of the scaled total charge $q_{N0}(t; D)$, obtained by formula (23) is about $\Delta_q = 0.0324$, where $\Delta_q = \max_{t\in[0,T]}[q_{N0}(t; D) - q_{N1}(t; D)]$, and $q_{N1}(t; D)$ is the scaled total charge obtained by formula (12) (Model (N1)). By decreasing the the value of the length parameter $L > 0$ this deviation increases. Thus for $L = 3$, $\Delta_q = 0.0799$. This is due to the influence of the right total flux $\Phi_R(0, T)$. Further, when the proportionality condition $\kappa := D_r/D_o = z_0/z_r$ holds , (Assumption (A2)) results obtained by Model (N0) and Model (N1) are close, with the difference of the deviation $\Delta_q > 0$, as Fig. 5 shows. However, results corresponding to the case $\kappa := D_r/D_o \neq z_0/z_r$ show ($\star\star$ lines in figures) that the scaled total charge $q_{N1}(t; D)$ strongly depends on the diffusivity coefficient $D_r$.

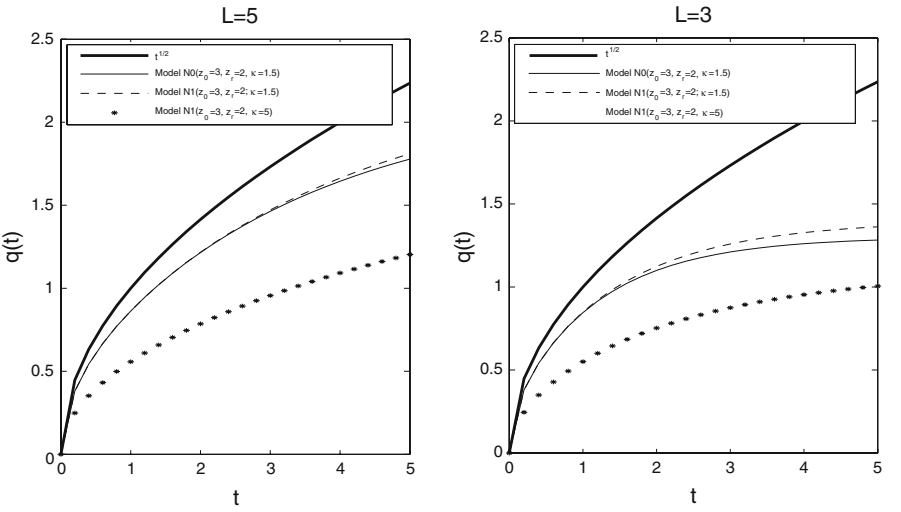


**Fig. 6** The scaled total charge $q(t)$ corresponding to different values of physical and geometric

## 6 Conclusions

In this paper, the nonlinear mathematical model of the ion transport problem, which includes diffusion and migration, is analyzed. This model is free from the assumptions (A1) and (A2). Some qualitative properties of the concentration function and fluxes are obtained. Precise physico–chemical meaning of these results are explained. The method of reducing the identification problem to the initial-boundary problem for strongly nonlinear parabolic equation is derived. Based on this method a numerical iteration algorithm for solving the nonlinear identification problem is proposed. The theoretical results have been validated by computational experiments, using real physical parameters. The presented computational results are consistent with their physical meaning and experimental results for real systems.

**Acknowledgments** The research has been supported by the Scientific and Technological Research Council of Turkey (TUBITAK) through the project Nr 108T332. The authors thank anonymous referees for reading the manuscript and their valuable suggestions which improved the revised version of the manuscript.

## References

1. A.J. Bard, L.R. Faulkner, *Electrochemical Methods* (Wiley, New York, 1980)
2. J.C. Myland, K.B. Oldham, Electrochem. Commun. **6**, 344 (2004)
3. B. Vuillemin, O. Bohnke, Solid State Ionics **68**, 257 (1994)
4. D. Pedone, M. Armand, D. Deroo, Solid State Ionics **28**(30), 1729 (1987)
5. F. Lantelme, H. Groult, N. Kumagai, Eloctrochim. Acta **45**, 3171 (2000)
6. L.K. Bieniasz, Eloctrochem. Commun. **4**, 917 (2002)
7. A.V. Churikov, A.V. Ivanischev, Eloctrochim. Acta **48**, 3677 (2003)
8. M.A. Vorotyntsev, M.D. Levi, D. Aurbach, J. Electroanal. Chem. **572**, 299 (2004)
9. S. Cohn, K. Pfabe, J. Redepenning, Math. Mod. Methods Appl. Sci. **3**, 445 (1999)
10. A. Hasanov, Math. Methods Appl. Sci. **21**, 1195 (1998)

11. A. Hasanov, J. Mueler, S. Cohn, J. Redepenning, Comput. Math. Appl. **39**, 225 (2000)
12. A. Hasanov, Ş. Hasanoglu, J. Math. Chem. **42**, 741 (2007)
13. A. Hasanov, Ş. Hasanoglu, J. Math. Chem. **44**, 731 (2008)
14. A. Hasanov, Ş. Hasanoglu, B. Pektaş, J. Math. Chem. (2009) (to appear)
15. A.A. Samarskii, *The Theory of Difference Schemes* (Marcel Dekker, New York, 2001)
16. R.P. Buck, M.B. Madaras, R. Mäckel, J. Electroanal. Chem. **366**, 55 (1994)